sustainability

MDPI

Article

Multi-Period Optimal Transmission Switching with Voltage Stability and Security Constraints by the Minimum Number of Actions

Mei Zhang [1], Lei Wang [2,*], Jiantao Liu [2,3], Xiaofan Deng [4] and Ke Wu [2]

[1] State Key Laboratory of Operation and Control of Wind Energy & Storage Systems, China Electric Power Research Institute, Beijing 100192, China; zhangmei@epri.sgcc.com.cn
[2] School of Electrical and Electronic Engineering, Shandong University of Technology, Zibo 250061, China; jiantaoliu777@163.com (J.L.); kewusdut@163.com (K.W.)
[3] Heze Power Supply Company of State Grid, Shandong Electric Power Company, Heze 274000, China
[4] Jiaxiang Power Supply Company of State Grid, Shandong Electric Power Company, Jining 314100, China; 17853309114@163.com
* Correspondence: wl7811@163.com

Abstract: Due to the ever-growing load demand and the deregulation of the electricity market, power systems often run near the stability boundaries, which deteriorates system voltage stability and raises voltage issues for the stable operations of power systems. Transmission switching (TS) has been applied to improve economic benefits and security operations for many applications. In this paper, a multi-period voltage stability-constrained problem (MP-VSTS) is established, intending to improve voltage security and the stability of a power system. Considering the online application of transmission switching, the minimum number of switching actions is taken as the objective function of the proposed MP-VSTS problem, which extends the TS application for real industries. The proposed model provides the switching lines for the upcoming period and the state of power systems for several successive periods. To overcome the solving difficulties of the proposed model, a two-stage approach is presented, which balances speed and accuracy. Numerical studies on the IEEE 118- and 662-bus power systems have demonstrated the proposed approach's performance.

Keywords: multi-period transmission switching; static voltage stability; voltage security; load margin; the minimum number of actions

Citation: Zhang, M.; Wang, L.; Liu, J.; Deng, X.; Wu, K. Multi-Period Optimal Transmission Switching with Voltage Stability and Security Constraints by the Minimum Number of Actions. *Sustainability* **2024**, *16*, 8272. https://doi.org/10.3390/su16188272

Academic Editor: Antonio Formisano

Received: 5 August 2024
Revised: 10 September 2024
Accepted: 19 September 2024
Published: 23 September 2024

1. Introduction

Contemporary power systems have undergone significant changes on the source side, power grid, and load side, such as changes in sources from traditional thermal generators to renewable energy units, which leads to the deficiency of reactive power. With the increasing load demand and competitive electricity market, power systems often operate around the stable boundary and under the higher stressful condition. Hence, voltage instability and the decrease of voltage support capability issues should be considered and taken more and more seriously for the stable operation of power systems. Generally, voltage instability often occurs at a low level of voltage magnitude, as shown with case 1 in Figure 1. It is reported that the drop in voltage magnitude and voltage instability happen frequently in power systems. The over-voltage issue in AC grids is studied in [1], and the variable reactance technique is proposed to mitigate voltage violation in transformers under both heavy and light loading conditions. More and more studies indicate that voltage instability may even occur at a high voltage level [2]. In other words, power systems may lose voltage stability before the bus voltage magnitude falls below voltage-secure level (e.g., 0.9 p.u.), as shown with case 2 in Figure 1, which is explained in Section 2. To sum up, it is of importance to consider voltage security and voltage stability (especially long-term voltage stability) for the security operation.

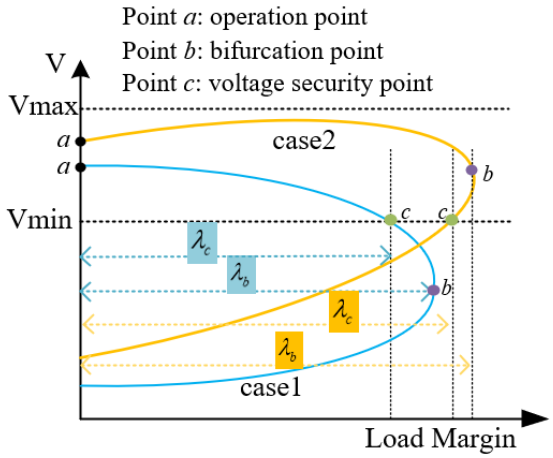

Figure 1. Illustration of voltage stability and security operation by P-V curves of two cases.

Traditionally, the power grid topology is fixed and precomputed according to the predicted day-ahead load demands and generation schedules. As a matter of fact, many studies have demonstrated that transmission switching (TS) is a powerful control with significant advantages in economics (without extra investment), flexibility, convenience (without complex control operations), and effectiveness [3,4]. From the perspective of TS applications, it has been applied in relieving transmission line overloading [5,6], minimizing the generation cost and transmission loss [7,8], improving the voltage profile [9], enhancing the stability of a power system [10–12], improving the economy [13] and reliability [14] of power systems, and reducing short-circuit currents [15]. In real industries, TS can provide a perfect option for system operators to deal with the overloading and voltage over-limit issues [16]. The cost of topology control for European networks can be reduced by between 0.30% under heavy net-loading conditions and 2.03% under light net-loading conditions [17]. In our previous studies, we determined that switching lines out from the current network topology can improve the load margin to the static voltage stability by 7.03% using single-line switching and 55% using multiple-line switching in an IEEE 118-bus power system and 12.26% in a large-scale power system [12]. Besides the base case, TS performed excellently in the N-1 contingency cases also. The load margin can be improved by 1.64% for the base case and 26.62% for the most critical contingency case [18]. Even for the uncertainties from renewable energy sources and loads, TS can also handle a certain degree of prediction error; that is, the TS solutions under the predicted outputs of renewable energy sources and loads can handle a relatively small fluctuation range of uncertainties [19] because the switching action can be a step change for power systems [20]. Based on the above studies, the predictive errors of the uncertainties in a relatively short-term time scale can be ignored in a TS problem. However, the above TS studies focus on the TS performance and method at a certain time moment, and how to find the TS solutions and performance during a long time period is not discussed.

In the literature, the approaches of solving TS problems within a reasonable time period can be classified into two types. One is to solve it for a relatively long time scale, for example, 24 h. The approaches can provide the day-ahead TS solutions for optimizing the day-ahead network topology for different purposes. In [21], a time-partition method based on day-ahead loading and renewable power outputs is developed to partition 24 h into several time periods. In each time period, a suitable network topology for the distribution system is identified to support the desired renewable integration requirement. The method is extended to power systems to ensure enough load margin to the static voltage stability limit [22]. In addition, TS is a very popular control that co-operates with other controls, such as optimal power flow (OPF) and unit commitment (UC), within a long time period. For example, the co-optimized UC and TS over 24 h are employed on European grids with renewable power [17]. In [23], TS is united with UC to reduce the generation cost, in which TS can provide benefits by reducing the volatility of wind power and the generation cost.

In recent years, many approaches have been presented to speed up the computation time. In [24], a real-time switching heuristic method based on neural networks is developed and can provide almost instant switching actions. A genetic algorithm for an ACOPF-based OTS problem is developed to better search the solution space in [25]. However, the above TS problems are all solved at a fixed time or time period (several hours) with the following disadvantages: (1) TS solutions using the above methods are solved based on the day-ahead predicted data (including loads and renewable outputs) or the worst scenario, which may be relatively conservative; (2) TS solutions for the fixed time or a time period do not consider the system states of two adjacent time. Hence, the solutions only apply to a single time, so the number of TS actions for the whole time periods may be too much, which is potentially 'unfriendly' for system operators.

With respect to the multiple TS solutions, several works have investigated the multiple TS solutions issue [26–28], which indicates that the different TS solutions with different numbers of switching actions may exist and contribute to the same objective, for example, the same generation cost. In [27], a two-stage optimization method is developed to reduce the generation cost, which demonstrates that multiple TS solutions serve the same generation cost. According to our experience, regarding TS in [12,18], the same TS solutions for the same load margin to the steady-state voltage stability limit also exist. For example, the load margin to steady-state voltage stability limit is 2.161 p.u. by switching 47–49 and 38–37 out and by only switching 37–40 out in example 2 in [18]. In addition, a switching line solution group exists; that is, there is a group of switching solutions in which the solutions with different numbers of switching lines serve the approximately equal load margins. However, from the point of view of practical TS application, system operators prefer the minimum number of operation actions. The reasons are that (1) system operators need enough operation time for switching lines out/in from power systems; too many switching actions may increase the operating time and complexity, and (2) they may trigger the electromechanical transient and electromagnetic transient issues if too many lines are switched from the power network, because the switching operations represent the step changes to some extent, being similar to contingency [21]. Hence, the fewer switching solutions with the similar objective are more practical than the global solutions with the optimal objective.

This paper focuses on multi-period static voltage security and stability-constrained transmission switching (MP-VSTS) to ensure enough load margin to the static voltage stability and security limit. In this study, the outputs of generators are assumed to be unchanged. To extend the online application of transmission switching for industries, the minimum number of switching actions is considered as the objective function in the proposed problem. The proposed MP-VSTS problem is solved in a rolling horizon, as shown in Figure 2, which is interpreted in Section 2.

In particular, the contributions of this paper are as follows:

- To demonstrate the necessity of incorporating both voltage stability and voltage security constraints, a modified IEEE 14-bus power system with detailed data is presented to show the two cases to voltage stability and voltage security limits, which demonstrates the necessity of the voltage stability and voltage security in the proposed MP-VSTS problem.
- A rolling multi-period transmission switching scheduling strategy is developed to overcome the difficulties of single-period optimal transmission switching issue, whose solution gives consideration both to the requirements of the upcoming time period and several future time periods.
- A multi-period MP-VSTS formulation is established to ensure a sufficient load margin by switching lines in a rolling horizon for power systems. The distinguishing feature of the proposed formulation is that the exact AC power flow equations and AC continual power flow equations are included instead of the linearized DC power flow equations and simplified voltage stability index.

- An effective two-stage approach is proposed to solve the proposed MP-VSTS problem, which balances speed and accuracy. In the first stage, a sensitivity-based method is presented to fast screen all the switching candidates. In the second stage, an iterative process is developed to solve the large-scale mixed-integer nonlinear programming problem to obtain the switching line solution for the upcoming time period.

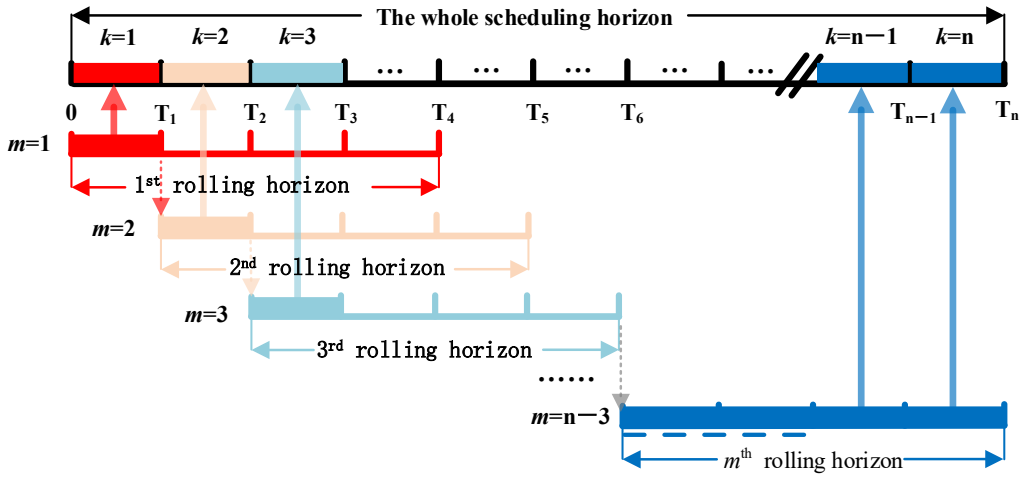

Figure 2. The schematic diagram of multi-period transmission switching scheduling based using rolling horizon strategy.

The structure of this paper is as follows: Section 2 interprets the idea of multi-period transmission switching with the voltage stability and security constraints. Section 3 formulates the mathematic model of the proposed MP-VSTS problem and presents the overall architecture of the proposed method and the detailed numerical steps. Numerical studies on the IEEE 118-bus and 662-bus power systems are discussed in Section 4. Section 5 concludes this paper.

2. MP-VSTS Problem Formulation

2.1. Explanation of the Necessity of Voltage Security and Stable Constraints

To interpret the necessity of incorporating both the voltage stability and voltage security constraints into the proposed MP-VSTS problem. P-V curves of two cases are used to denote the two possible operation situations in power systems, as shown in Figure 1. Point a denotes the operation point of the power system, corresponding to the solution of power flow equations; point b denotes the voltage bifurcation point; and point c is the voltage security point, which indicates the point to the minimum voltage magnitude limit (say 0.9 p.u.) of the maximum voltage magnitude limit (say 1.1 p.u.). The voltage magnitude upper/lower bounds are often defined by system operators according to the secure operation requirements of power systems:

- Case 1: Generally, in some situations, the voltage security limit may be reached before the voltage collapse point (i.e., the voltage bifurcation point, point b), as shown with the P-V curve of case 1 in Figure 1. Hence, the load margin to the voltage stability and security limit is $\lambda = \lambda_C$, where λ_C is the distance between the operation point (point a) and the voltage security point (point c). This situation is quite common in power systems.
- Case 2: In other situations, the voltage bifurcation point (point b) may be reached before the voltage magnitude reaches the voltage security limit (point c), as shown with the P-V curve of case 2 in Figure 1. Hence, the load margin to the voltage stability and security limit is $\lambda = \lambda_b$, where λ_b is the distance between the operation point (point a) and the voltage bifurcation point (point b). To show this, the authors performed the simulations on a modified IEEE 14-bus power system, whose detailed data of the example are listed in Tables 1 and 2 and whose diagram is shown in Figure 3. The

continuation power flow method is employed to calculate the exact load margin to the static voltage stability limit. The load margin of this case is computed as 194 MW (i.e., $\lambda_{base} = 1.2985$) along with the active and reactive power variations listed in Table 3. The P-V curves of all PQ buses are plotted in Figure 4.

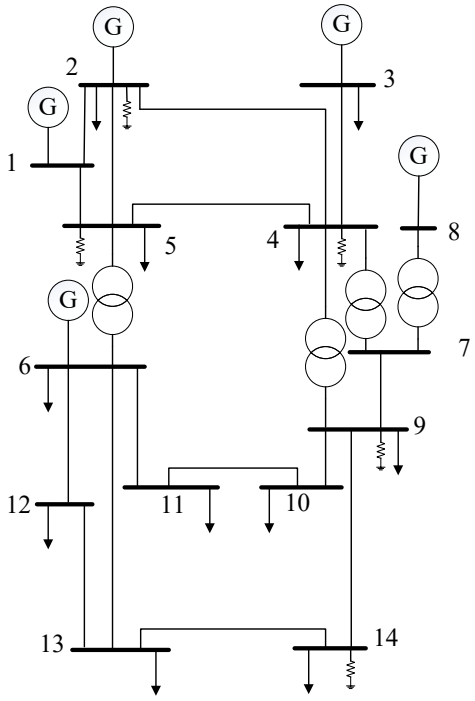

Figure 3. The diagram of the modified IEEE 14-bus power system.

Table 1. The branch data of the modified IEEE 14-bus power system.

No.	From Bus	To Bus	Resistance (p.u.)	Reactance (p.u.)	Admittance (p.u.)	Non-Standard Ratio of Transformer
1	2	5	0.05695	0.17388	0.034	-
2	6	12	0.12291	0.25581	0	-
3	12	13	0.22092	0.19988	0	-
4	6	13	0.06615	0.13027	0	-
5	6	11	0.09498	0.19890	0	-
6	11	10	0.08205	0.19207	0	-
7	9	10	0.03181	0.08450	0	-
8	9	14	0.12711	0.27038	0	-
9	14	13	0.17093	0.34802	0	-
10	7	9	0	0.11001	0	-
11	1	2	0.01938	0.05917	0.0528	-
12	3	4	0.06701	0.17103	0.0346	-
13	1	5	0.05403	0.22304	0.0492	-
14	5	4	0.01335	0.04211	0.0128	-
15	2	4	0.05811	0.17632	0.0374	-
16	5	6	0	0.25202	-	0.932
17	4	9	0	0.55618	-	0.969
18	4	7	0	0.20912	-	0.978
19	8	7	0	0.17615	-	0

The voltage magnitudes of all PQ buses at the bifurcation point are higher than 0.9 p.u., so it can be concluded that no voltage magnitude violations are encountered before the voltage collapse point (i.e., the voltage stability limit of this case is the limit factor instead of the voltage security limit). Based on the above numerical studies, the operational

limit for a power system cannot only be voltage magnitude violation but is also the voltage collapse. Therefore, the two constraints should be incorporated into the optimal operation decision of power systems.

Table 2. Power flow data of the modified IEEE 14-bus power system.

Bus	Shunt (p.u.)	Voltage		Generator		Load	
		Magnitude	Phase Angle (Degree)	Active Power	Reactive Power	Active Power	Reactive Power
1	-	1.06	0	2.4801	0.5679		
2	0.4	1	−0.0709	0.4000	−1.5516	0.217	0.127
3	-	1	−0.4308		0.4874	0.942	0.19
4	0.6	1.0256	−0.2522			0.478	0.04
5	0.93	1.0331	−0.2063			0.076	0.016
6	-	1	−0.3015		−0.6170	0.112	0.075
7	-	1.0397	−0.3106				
8	-	1	−0.3106		−0.2253		
9	0.4	1.0612	−0.3409			0.295	0.166
10	-	1.0427	−0.3401			0.090	0.058
11	-	1.0181	−0.3247			0.035	0.018
12	-	0.9988	−0.3221			0.061	0.016
13	-	1.0065	−0.3331			0.135	0.058
14	0.4	1.0853	−0.3853			0.149	0.050

Table 3. The real and reactive generation/load variations.

Generation /Load	Bus	Increased Direction (p.u.)	
		ΔP	ΔQ
Generation	6	0.80676	
	8	0.53784	
Load	2	0.36	0.135
	3	0.864	0.270
	11	0.270	0.081

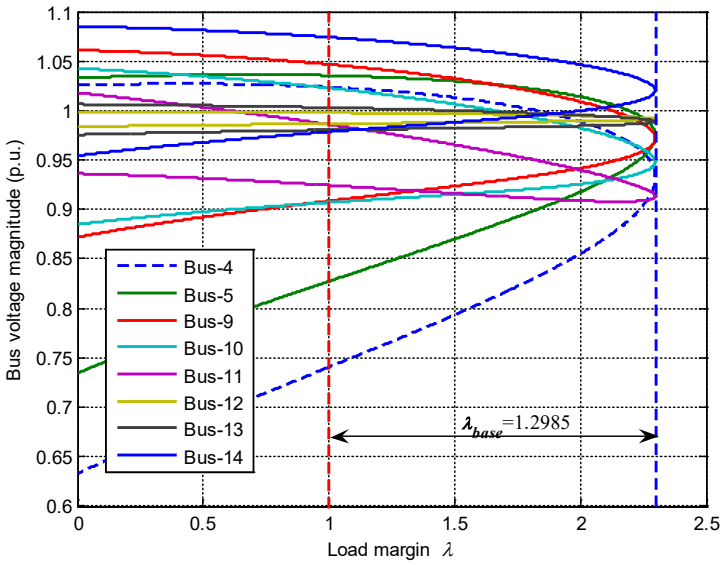

Figure 4. P-V curves of the modified IEEE 14-bus power system.

2.2. Architecture of the Proposed MP-VSTS Problem

The traditional single-period optimal scheduling of power systems usually focuses on the optimal solution for the immediate time but fails to be optimal for the successive

time periods. A multi-period transmission switching rolling scheme is developed in this paper, which can be observed in Figure 2. Compared with the redispatch of generators, a switching line is a kind of action with a relatively large step change on the operating state of the power system. Hence, in the proposed MP-VSTS rolling strategy, the time resolution can be relatively long, say one hour for each time period, instead of a 15 min resolution for the generator's dispatch problem. Therefore, the look-ahead schedule module for the MP-VSTS problem is one hour of time resolution with a rolling horizon/window every 4 h.

The necessary input data for the proposed rolling MP-VSTS problem include the current system states (i.e., voltage magnitude and phase angle, line current, generator outputs, and the load demands) and the data of the upcoming time period (i.e., the load demands and generator schedule for the upcoming time period (see one hour) and the three following time periods). The solved transmission line status of the upcoming time period serves as the solution and is sent to system operators to implement. The transmission line solutions of the three other time periods serve as the initial point for the next rolling cycle. The presented MP-VSTS problem is solved as in receding horizon control, as shown in Figure 2.

Another important issue is raised regarding the real application of transmission switching in industries. Line switching cannot be conducted frequently, and the system operators prefer the least actions to maintain the stable and secure operation of power systems. Hence, in this paper, the number of switching lines for operators to operate is considered and established as the objective function of the proposed MP-VSTS problem.

2.3. Formulation of the Proposed MP-VSTS Problem

The proposed MP-VSTS problem seeks to identify the minimum number of switching lines to ensure enough voltage stability margin (i.e., load margin) in the entire rolling time domain. Hence, the MP-VSTS problem can be stated as follows:

$$\min \sum_{t=1}^{T} \sum_{ij \in \Omega_{L,t}} \left(1 - Z_{ij,t}\right) \tag{1}$$

$$s.t. \begin{cases} P_{i,t}^{g} - P_{i,t}^{d} = V_{i,t} \sum\limits_{j \in i} V_{j,t} [(G_{ij} \cos\theta_{ij,t} + B_{ij} \sin\theta_{ij,t}) Z_{ij,t}] \\ Q_{i,t}^{g} - Q_{i,t}^{d} = V_{i,t} \sum\limits_{j \in i} V_{j,t} [(G_{ij} \sin\theta_{ij,t} - B_{ij} \cos\theta_{ij,t}) Z_{ij,t}] \end{cases} \tag{2}$$

$$\begin{cases} P_{i,t}^{g} - P_{i,t}^{d} + \lambda_t d_{i,t}^{p} = V_{i,t}^{B} \sum\limits_{j \in i} V_{j,t}^{B} [(G_{ij} \cos\theta_{ij,t}^{B} + B_{ij} \sin\theta_{ij,t}^{B}) Z_{ij,t}] \\ Q_{i,t}^{g} - Q_{i,t}^{d} + \lambda_t d_{i,t}^{q} = V_{i,t}^{B} \sum\limits_{j \in i} V_{j,t}^{B} [(G_{ij} \sin\theta_{ij,t}^{B} - B_{ij} \cos\theta_{ij,t}^{B}) Z_{ij,t}] \\ d_{i,t}^{p} = \left(P_{i,t+1}^{g} - P_{i,t}^{g}\right) - \left(P_{i,t+1}^{d} - P_{i,t}^{d}\right) \\ d_{i,t}^{q} = \left(Q_{i,t+1}^{d} - Q_{i,t}^{d}\right) \end{cases}, t \in \{1, 2, \cdots, T-1\} \tag{3}$$

$$\lambda_t^{post} \geq \lambda_{th} \tag{4}$$

$$V_i^{min} \leq V_{i,t} \leq V_i^{max} \tag{5}$$

$$\theta_{ij}^{min} \leq \theta_{ij,t} \leq \theta_{ij}^{max} \tag{6}$$

$$\max\left(\left|S_{ij,t}\right|, \left|S_{ji,t}\right|\right) \leq S_{ij}^{max} \tag{7}$$

$$\sum_{m \in U_i(i)} Z_{im,t} \geq 1 \tag{8}$$

where t is the current time period; T is the number of periods in a rolling time horizon; $Z_{ij,t}$ is an integer variable representing the operating status of transmission line $i-j$ if the line $i-j$ is switched out from the network at the t^{th} time period $Z_{ij,t} = 0$; otherwise, the line $i-j$ is in service at $Z_{ij,t} = 1$; $\Omega_{L,t}$ is the set of transmission lines; $P_{i,t}^{g}$ and $Q_{i,t}^{g}$ are the active

and reactive power outputs of generators on bus i at the t^{th} time period; $V_{i,t}$ and $\theta_{ij,t}$ are the bus i voltage magnitude and its angle difference between buses i and j at the t^{th} time period, respectively; $G_{ij,t}$ and $B_{ij,t}$ are the conductance and susceptance of line $i-j$, respectively; $V_{i,t}^{B}$ and $\theta_{ij,t}^{B}$ are the voltage magnitude of bus i and voltage angle difference between buses i and j at the t^{th} time period, respectively; λ_t is the load margin at the t^{th} time period; λ_t^{post} is the load margin after line switching at the t^{th} time period; λ_{th} is a desirable load margin value; α_t is the load margin increase ratio at the t^{th} time period; V_i^{max} and V_i^{min} are the upper and lower limits of the voltage magnitude on bus i; θ_{ij}^{max} and θ_{ij}^{min} are the upper and lower limits of the voltage phase angle difference between bus i and j at the t^{th} time period; $S_{ij,t}$ and S_{ij}^{max} are the apparent power and its limit between bus i and j, respectively; $Z_{im,t}$ is the operating status of the m^{th} line connected on bus i at the t^{th} time period; and $U_t(i)$ is the set of buses connected to bus i at the t^{th} time period.

The objective function (1) is to minimize the number of switching actions to ensure that the load margin of all time periods in a rolling time horizon meets the expected requirements. Constraints (2) and (3) denote the AC power flow equations and AC continual power flow equations. Constraint (4) indicates the load margin requirement. Constraints (5)–(7) denote the operation constraints for the post-switching power system, including the voltage magnitude constraint (5), voltage phase angle constraint (6), and thermal limit constraint (7). Constraint (8) is used to avoid the occurrence of islands for a post-switching power system.

2.4. Difficulties of the Proposed MP-VSTS Problem

The constraints make the presented MP-VSTS problem (1)–(8) highly nonlinear, and it is a typical mixed-integer nonlinear programming (MINLP) problem that is hard to solve directly. The difficulties include the following: (1) Several time periods are involved in a rolling time horizon; hence, the solutions of each period in a rolling horizon need to not only decide for the upcoming period but also adapt to the other time periods, which results in the increasing number of constraints for multiple time periods and solving the proposed MP-VSTS problem difficultly and complicatedly. (2) The involvement of the nonlinear AC continuation power flow equations and the 0–1 decision variables further increases the difficulty for solving the proposed MP-VSTS problem, resulting in an excessively long computation time. In the following section, we develop a two-stage solution approach balancing the speed and accuracy. It should be noted that the developed approach is not devoted to finding the optimal TS solutions but rather the feasible solutions as soon as possible for system operators due to the practical application.

In the proposed MP-VSTS model, the 0–1 variable Z_{ij} is as a product term multiplying the nonlinear term of constraints (2) and (3). The conventional dealing method is the big-M method, which is suitable for linear constraints, such as DC power flow equations, but is not applicable to the nonlinear model. Therefore, we move the 0–1 variables from the nonlinear term to the bus admittance matrix and develop a transmission switching model based on the branch addition method. Taking the branch h as an example, the bus voltage equations of branch h can be expressed as

$$\begin{bmatrix} I_f^h \\ I_o^h \end{bmatrix} = \boldsymbol{Y}_{br}^h \begin{bmatrix} V_f^h \\ V_o^h \end{bmatrix} = \begin{bmatrix} \boldsymbol{Y}_{ff}^h & \boldsymbol{Y}_{fo}^h \\ \boldsymbol{Y}_{of}^h & \boldsymbol{Y}_{oo}^h \end{bmatrix} \begin{bmatrix} V_f^h \\ V_o^h \end{bmatrix} \tag{9}$$

where $\boldsymbol{Y}_{br}^h$ is the admittance matrix of the h^{th} branch; $\boldsymbol{Y}_{ff}^h$, $\boldsymbol{Y}_{fo}^h$, $\boldsymbol{Y}_{of}^h$, and $\boldsymbol{Y}_{oo}^h$ are the four partitioned matrixes of $\boldsymbol{Y}_{br}^h$; f and o are the first bus and the end bus of the h^{th} branch, respectively; I_f^h and I_o^h are the injected currents of bus f and bus o of the h^{th} branch, respectively; and V_f^h and V_o^h are the voltage magnitude of bus f and bus o of the h^{th} branch, respectively. Hence,

$$\boldsymbol{Y}_f = \mathrm{diag}\left[\boldsymbol{Y}_{ff}\right]\boldsymbol{C}_f + \mathrm{diag}\left[\boldsymbol{Y}_{fo}\right]\boldsymbol{C}_o \tag{10}$$

$$\boldsymbol{Y}_o = \text{diag}\left[\boldsymbol{Y}_{of}\right]\boldsymbol{C}_f + \text{diag}[\boldsymbol{Y}_{oo}]\boldsymbol{C}_o \tag{11}$$

$$\boldsymbol{Y}_{bus} = \boldsymbol{C}_f^T\boldsymbol{Y}_f + \boldsymbol{C}_o^T\boldsymbol{Y}_o + \boldsymbol{Y}_{sh} \tag{12}$$

where $\boldsymbol{Y}_f$ and $\boldsymbol{Y}_o$ are the admittance matrices of the first bus and the end bus of the h^{th} branch, respectively; ***diag***$[\cdot]$ is the diagonalization operator; $\boldsymbol{C}_f$ and $\boldsymbol{C}_O$ are the $N_L \times N_b$ dimensional connection matrices of bus f and bus o, respectively; $\boldsymbol{Y}_{sh}$ is an additional matrix of ground susceptance; and N_L and N_b are the numbers of transmission lines and buses, respectively.

Taking the single line $i-j$ switching as an example, the nature of the switching line $i-j$ is to change the elements (i.e., g_{ij} and b_{ij}) in the original admittance matrix. Therefore, the admittance matrix $\boldsymbol{Y}'_{bus}$ after the switching line $i-j$ can be expressed as the sum of the original admittance matrix $\boldsymbol{Y}_{bus}$ and the branch admittance change matrix $\Delta\boldsymbol{Y}_{ij}$ by (13)–(14):

$$\boldsymbol{Y}'_{\text{bus}} = \boldsymbol{Y}_{\text{bus}} + \Delta\boldsymbol{Y}_{ij} \tag{13}$$

$$\Delta\boldsymbol{Y}_{ij} = \boldsymbol{C}_{\text{b},ij}\text{diag}\left[-y_{ij}\left(1-Z_{ij}\right)\right]\boldsymbol{C}_{\text{b},ij}^{\text{T}} + \boldsymbol{C}_{\text{b}f,i}\text{diag}\left[-\text{j}b_{ij0}\left(1-Z_{ij}\right)\right]\boldsymbol{C}_{\text{b}f,i}^{\text{T}} + \boldsymbol{C}_{\text{b}o,j}\text{diag}\left[-\text{j}b_{ij0}\left(1-Z_{ij}\right)\right]\boldsymbol{C}_{\text{b}o,j}^{\text{T}} \tag{14}$$

where $\boldsymbol{C}_{b,ij}$ is the bus–branch association matrix; and $\boldsymbol{C}_{bf,i}$ and $\boldsymbol{C}_{bo,j}$ are the position vectors of bus i and bus j of line $i-j$, where $\boldsymbol{C}_{b,ij}$= $\boldsymbol{C}_{bf,i} - \boldsymbol{C}_{bo,j}$. When several lines are allowed to be switched out, the change in the admittance matrix can be extended according to (13)–(14).

3. Solution Methodology

3.1. Overall Architecture of the Proposed Decomposition Method

Due to the strong nonlinear characteristics of the MP-VSTS problem, a two-stage solution method is proposed to obtain the feasible solutions of a rolling time horizon within a reasonable time period. The two stages include the prescreening stage (stage 1) and the decomposition stage (stage 2). The tasks of the two stages are summarized as follows:

Stage 1 (the prescreening stage): To quickly solve the proposed problem, a prescreening method is employed to screen all the line candidates and reserve the possible effective switching lines for stage 2 for final identification.

Stage 2 (the decomposition stage): In this stage, the proposed MP-VSTS problem model is decomposed into two subproblems and solved iteratively, i.e., a MILP and an NLP subproblem, which will be explained below.

To clearly describe the solving process, the MP-VSTS problem formulation can be written in the following compact form:

$$\min\sum_{t=1}^{T}\sum_{ij\in\Omega_{\text{L},t}}\left(1-Z_{ij,t}\right) \tag{15}$$

$$s.t.\quad g(x_t, p_t) = 0 \tag{16}$$

$$h(x_t, p_t) \le 0 \tag{17}$$

$$g^{\text{B}}(x_t^{\text{B}}, p_t, \lambda_t) = 0 \tag{18}$$

$$h^{B}(x_t^{B}, p_t, \lambda_t) \le 0 \tag{19}$$

$$p_{ij,t} = Z_{ij,t}p_{ij,t}^{0}, Z_{ij,t} \in \{0,1\} \tag{20}$$

where $\text{g}(\cdot)$ and $\text{g}(\cdot)^{B}$ are the AC power flow equations and the AC continuation power flow equations; $h(\cdot)$ and $h(\cdot)^{B}$ are the inequality constraints; x_t is the state variables of post-switching power system at the t^{th} time period, including the voltage magnitude and phase angle; p_t is the control vector at the t^{th} time period, which is composed of all the transmission lines; and $p_{ij,t}$ and $p_{ij,t}^{0}$ are the transmission line $i-j$ parameters at the t^{th} time period.

3.2. The Proposed Two-Stage Solution Methodology

Stage 1: the prescreening stage

A prescreening technique based on a linear sensitivity method is employed to prescreen switching candidates whose disconnection can increase the load margin to the static voltage stability limit. The compact AC continuation power flow equations can be written as follows:

$$g(x, p, \lambda) = 0 \tag{21}$$

At the bifurcation point (x^*, λ^*), there exists a nonzero vector ω orthogonal to the Jacobian matrix J, i.e., $\omega J = 0$,

$$J = [g_x]|^T_{(x_*, \lambda_*)} \tag{22}$$

$$\Delta\lambda = \frac{-\omega[g_p]|^T_{(x_*, \lambda_*)}}{\omega[f_\lambda]|^T_{(x_*, \lambda_*)}} \Delta p = S_p \Delta p \tag{23}$$

where g_x is the derivatives of (21) with respective to x; g_p is the derivatives of (21) with respective to p; g_λ is the derivatives of (21) with respective to λ; and $\Delta\lambda$ is the change in the load margin, which can be estimated using (23). Therefore, the change in the load margin due to switching line $i - j$ out is

$$\Delta\lambda_{ij,t} = S_p \Delta p_{ij} \tag{24}$$

where Δp_{ij} is the negative parameter of line $i - j$. $\Delta\lambda_{ij,t} > 0$ indicates that switching line $i - j$ out may increase the load margin; otherwise, the load margin may be decreased. After the prescreening stage, the candidates for 0–1 integer variables of each period are reduced from 2^{N_l} to $2^{N^1_L}$, where N^1_L is the total number of elements of the candidate line set $\Omega^1_{L,t}$. After the prescreening stage, $\Omega^1_{L,t}$ is sent to stage 2.

Stage 2: the decomposition stage

The proposed MP-VSTS problem is a typical MINLP problem that is difficult to solve directly. In this stage, the proposed MP-VSTS model is decomposed into a MILP subproblem and an NLP subproblem. The MILP subproblem is to determine the possible TS solutions using a linearized model. The NLP subproblem aims to obtain a slack TS subproblem solution (the solutions are continuous variables between 0 and 1) with the nonlinear AC power flow equations and AC continuation power equations. The two subproblems are solved iteratively till the solutions of these two subproblems are converged. The two subproblems are MILP and NLP which can be solved using the available commercial solver.

MILP subproblem

The MILP subproblem determines the possible TS solutions of a rolling horizon (4 time periods in this paper) with the objective of minimizing the solution difference of the two subproblems. Before constructing the MILP model, a continuation power flow tool is employed to obtain the load margin of the pre-switching base case and the system states (including the voltage magnitude and phase angle). The MILP subproblem is subject to the linearized constraints of the equalities and the inequalities in (15)–(20) according to the states at the bifurcation point. The MILP subproblem formulation can be listed in the following form (25)–(31):

$$\min \sum_{t=1}^{T} \sum_{ij \in \Omega^1_{L,t}} \left| \overline{Z}^k_{ij,t} - Z^k_{ij,t} \right| \tag{25}$$

$$s.t. \quad g\left(\overline{x}^k_t, \overline{p}^k_t\right) + \nabla g\left(\overline{x}^k_t, \overline{p}^k_t\right) \left[x_t - \overline{x}^k_t \quad p_t - \overline{p}^k_t\right]^T = 0 \tag{26}$$

$$h\left(\overline{x}^k_t, \overline{p}^k_t\right) + \nabla h\left(\overline{x}^k_t, \overline{p}^k_t\right) \left[x_t - \overline{x}^k_t \quad p_t - \overline{p}^k_t\right]^T \leq 0 \tag{27}$$

$$g^{\mathrm{B}}\left(\overline{x}^{\mathrm{B},k}_t, \overline{p}^k_t, \overline{\lambda}^k_t\right) + \nabla g^{\mathrm{B}}\left(\overline{x}^{\mathrm{B},k}_t, \overline{p}^k_t, \overline{\lambda}^k_t\right) \left[x^{\mathrm{B}}_t - \overline{x}^{\mathrm{B},k}_t \quad p_t - \overline{p}^k_t \quad \lambda_t - \overline{\lambda}^k_t\right]^T = 0 \tag{28}$$

$$h^{\mathrm{B}}\left(\overline{x}_t^{\mathrm{B},k}, \overline{p}_t^k, \overline{\lambda}_t^k\right) + \nabla h^{\mathrm{B}}\left(\overline{x}_t^{\mathrm{B},k}, \overline{p}_t^k, \overline{\lambda}_t^k\right)\left[x_t^{\mathrm{B}} - \overline{x}_t^{\mathrm{B},k} \quad p_t - \overline{p}_t^k \quad \lambda_t - \overline{\lambda}_t^k\right]^T \le 0 \tag{29}$$

$$\sum_{ij \notin \Phi_t} Z_{ij,t} - \sum_{ij \in \Phi_t} Z_{ij,t} \le N_{\mathrm{L},t}^1 - 1 \tag{30}$$

$$p_{ij,t} = Z_{ij,t} p_{ij,t}^0, Z_{ij,t} \in \{0,1\} \tag{31}$$

where k is the number of iterations; $\nabla \mathrm{g}(\cdot)$ and $\nabla \mathrm{g}^B(\cdot)$ are the Jacobian matrixes of the equality constraints $\mathrm{g}(\cdot)$ and $\mathrm{g}^B(\cdot)$, respectively; $\left(\overline{x}_t^k, \overline{p}_t^k, \overline{\lambda}_t^k, \overline{Z}_t^k\right)$ denote the feasible solutions of the NLP subproblem; and $\overline{Z}_{ij}^k$ is the integer vector representing the transmission line $i-j$ state in the NLP subproblem (which is solved in the NLP subproblem) $\overline{Z}_{ij}^k \epsilon \overline{Z}_t^k$. $\sum_{ij \notin \Phi_t} Z_{ij,t} - \sum_{ij \epsilon \Phi_t} Z_{ij,t} < N_{L,t}^1 - 1$ is employed to avoid the endless loop during solving the MILP subproblem and $\Phi_t = \left\{ij : \overline{Z}_{ij}^k = 0\right\}$.

Obviously, the above model (25)–(31) is a non-convex optimization programming problem, and the objective function can be converted to (32) by introducing the auxiliary variable η_{ij}. After that, the MILP subproblem is ultimately transformed into a convex optimization problem, which can be directly solved using a linear solver.

$$\min \sum_{t=1}^{T} \sum_{ij \in \Omega_{\mathrm{L},t}^1} \eta_{ij,t} \tag{32}$$

$$s.t. \ -\eta_{ij,t} \le \overline{Z}_{ij,t}^k - Z_{ij,t}^k \le \eta_{ij,t} \tag{33}$$

$$\eta_{ij,t} \ge 0 \tag{34}$$

NLP subproblem

The NLP subproblem can be listed in the following form (35)–(40) after the 0–1 integer variables are relaxed to the 0–1 continuous variables:

$$\min \sum_{t=1}^{T} \sum_{ij \in \Omega_{\mathrm{L},t}^1} \left| Z_{ij,t}^k - \overline{Z}_{ij,t}^k \right| \tag{35}$$

$$s.t. \ \ g\left(\overline{x}_t^k, \overline{p}_t^k\right) = 0 \tag{36}$$

$$h\left(\overline{x}_t^k, \overline{p}_t^k\right) \le 0 \tag{37}$$

$$g^{\mathrm{B}}\left(\overline{x}_t^{\mathrm{B},k}, \overline{p}_t^k, \overline{\lambda}_t^k\right) = 0 \tag{38}$$

$$h^{\mathrm{B}}\left(\overline{x}_t^{\mathrm{B},k}, \overline{p}_t^k, \overline{\lambda}_t^k\right) \le 0 \tag{39}$$

$$\overline{p}_{ij,t} = \overline{Z}_{ij,t} \overline{p}_{ij,t}^0 \tag{40}$$

where $\overline{Z}_{ij,t}^k$ is a continuous variable between 0 and 1 denoting the state of line $i-j$ at the t^{th} time period and the k^{th} iteration. In (35), if $Z_{ij,t}^k = 1$, $|\overline{Z}_{ij,t}^k - Z_{ij,t}^k| = 1 - \overline{Z}_{ij,t}^k$; otherwise, $|\overline{Z}_{ij,t}^k - Z_{ij}^k| = \overline{Z}_{ij,t}^k$. Then the objective function in (35) can be replaced by the convex function shown in (41). Hence, it can be solved directly using the available NLP methods (such as the IPM method) or NLP solvers.

$$\min \sum_{i,j \in \Phi} \overline{Z}_{ij,t}^k + \sum_{i,j \notin \Phi} \left(1 - \overline{Z}_{ij,t}^k\right) \tag{41}$$

To deal with the relaxed integer variables, we propose a strategy combining the round-off technique and the sensitivity (24) according to (42).

$$\overline{Z}_{ij,t}^{k} = \begin{cases} 0 & \overline{Z}_{ij,t}^{k} < 0.5,\ \Delta\overline{\lambda}_{ij,t}^{k} > 0 \\ 1 & \text{other} \end{cases} \tag{42}$$

3.3. Numerical Steps

The numerical steps of the proposed two-stage strategy are sketched as below, whose flow chart is shown in Figure 5.

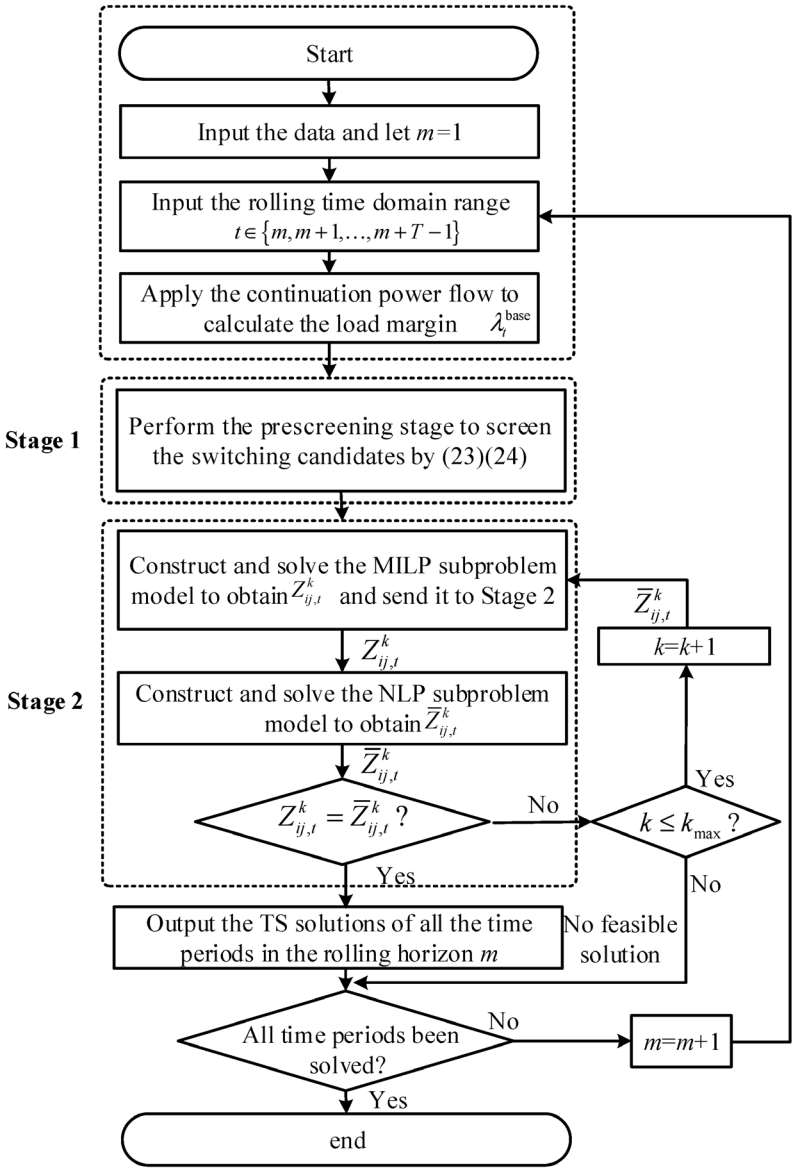

Figure 5. Flow chart of the proposed solution method.

Step 1: Input the necessary data for the MP-VSTS problem, including the current network topology, the generation schedules, the operation states (say from the state estimator), and the load margin requirement; input the rolling time domain range $t \in \{m, m+1, \ldots m+T-1\}$ and the line-switching candidates. Let $m = 1$.

Step 2: Apply a continuation power flow tool to compute the load margins λ_t^{base} of pre-switching power systems of each period in the whole rolling horizon.

Step 3 (the prescreening stage): Calculate the sensitivities of all the switching candidates using (24). Select the switching lines with the positive sensitivity, that is, the lines

that contribute to increasing the load margins, from the candidate line set $\mathbf{\Omega}_{L,t}^{1}$, and send them to step 4. Let $k = 1$, and input the maximum number of iterations k_{max}.

Step 4: Construct the MILP subproblem model according to the information at the bifurcation point calculated in step 3 according to (25)–(34). Solve the MILP subproblem using the available commercial solver, and send the solution Z_t^k to the next step.

Step 5: Construct the NLP subproblem model according to (35)–(42). Solve the NLP subproblem to obtain the integer solutions $\overline{Z}_t^k$.

Step 6: If $\overline{Z}_t^k = Z_t^k$ and $k < k_{max}$, the switching line solutions are found; go to step 7; otherwise, let $k = k + 1$, and go back to step 4.

Step 7: Output the TS solutions of all the time periods in the whole rolling horizon. Send the TS solutions for the upcoming time period to the system operators, and send the TS solutions for the other time periods to the next rolling horizon as the initial guess. Let $m = m + 1$, and go back to step 2.

4. Results and Discussion

The proposed MP-VSTS problem and two-stage method are evaluated on the IEEE 118-bus [29] and the 662-bus power systems. The proposed two-stage method is implemented in MATLAB2018bm. The solvers for the MILP and NLP subproblems are Gurobi and Bonmin, respectively.

4.1. Example 1

The test is performed in the IEEE 118-bus power system, which consists of 186 transmission lines with total active and reactive loads of 4242 MW and 1438 Mvar, respectively. A total of 39 loads at buses #33–#36, #39–#60, #62, #66–#67, #76–#80, #97–#99, #116, and #118 are increased, and the rests remain unchanged. The generators on buses #1, #4, and #31 are scheduled to supply the increasing loads. Here, $\lambda_{th} = 2550$ MW.

The load margins of the pre-switching power system at each time period are shown in Figure 6, in which the load margins of periods #5–#9 and #11–#12 do not meet the requirement. Taking period #5 as an example, 34 switching lines with positive sensitivities are selected using (19) after the prescreening stage and sent to stage 2. In this stage, the number of the integer variables is reduced from 2^{175} to 2^{34}. Transmission lines with the top 10 sensitivities are listed in Table 4. In stage 2, the TS solutions of the MILP and NLP subproblems of each iteration are listed in Table 5. The iterative solving process is converged after two iterations. The changes in the control variables in these two iterations are listed in Table 6. In the MILP subproblem, 11 out of 34 candidate transmission lines obtained in stage 1 are selected and sent to the NLP subproblem. After the NLP subproblem, the switching lines, including 1–3 and 31–32, are rounded to 0. In the second iteration, the solutions of the MILP subproblem and the NLP subproblem are converged, and the iteration terminates. The final solution is line 31–32.

Applying the proposed two-stage method for the whole 12 h, the transmission line switching schemes for each period are shown in Table 7. The load margins of each time period before and after transmission switching are shown in Figure 7.

Table 4. The top 10 switching lines of period #5 in IEEE 118-bus power system.

Switching Lines	Sensitivity	Switching Lines	Sensitivity
17–31	10.5293	2–12	2.0216
31–32	4.8266	8–30	1.9530
1–3	4.6048	32–113	1.8210
1–2	3.6998	15–17	1.6247
3–5	3.4171	3–12	1.5856

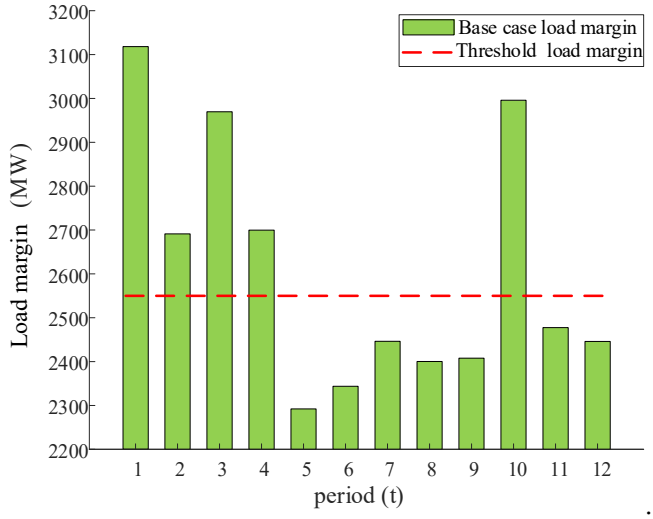

Figure 6. Load margins of the pre-switching power system at each time period in the 118-bus power system.

Table 5. TS solutions of each iteration in IEEE 118-bus power system.

k	Problem	Line No.	Switching Lines
1	MILP	2, 3, 4, 21, 23, 29, 37, 39, 42, 116, 180	1–3, 4–5, 3–5, 15–17, 17–18, 22–23, 8–30, 17–31, 31–32, 69–75, 32–113
	NLP	2, 42	1–3, 31–32
2	MILP	42	31–32
	NLP	42	31–32

Table 6. Changes in 0–1 integer variables in IEEE 118-bus power system.

k	Problem	Z_2	Z_3	Z_4	Z_{21}	Z_{23}	Z_{29}	Z_{37}	Z_{39}	Z_{42}	Z_{116}	Z_{180}
1	MILP	0	0	0	0	0	0	0	0	0	0	0
	NLP	0.181	1	1	1	1	1	1	1	0.029	1	1
2	MILP	1	1	1	1	1	1	1	1	0	1	1
	NLP	1	1	1	1	1	1	1	1	0.132	1	1

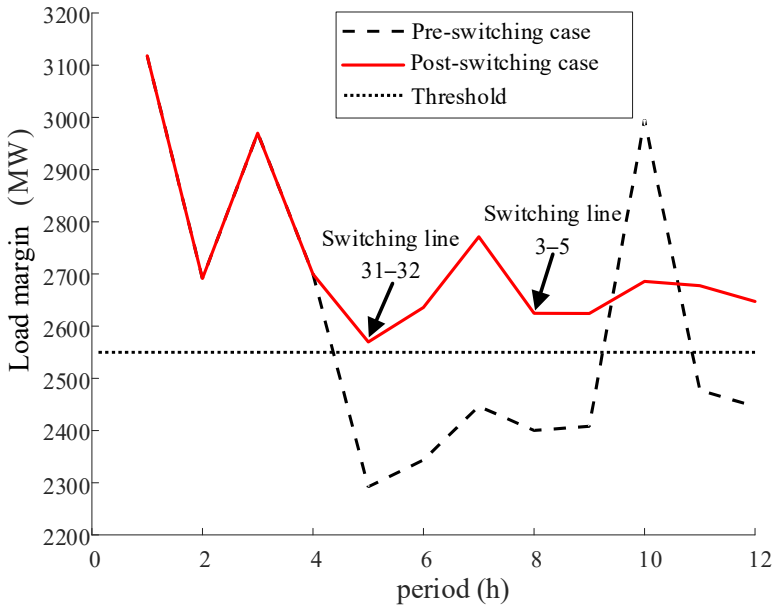

Figure 7. Load margins before and after transmission switching of each period in Example 1.

Table 7. Transmission line switching schemes for each period of IEEE 118-bus power system.

Line	Transmission Line Status (Hour)											
	1	**2**	**3**	**4**	**5**	**6**	**7**	**8**	**9**	**10**	**11**	**12**
3–5	1	1	1	1	1	1	1	0	0	0	0	0
31–32	1	1	1	1	0	0	0	0	0	0	0	0

In this example, the proposed method has been implemented for 12 h, and there are a total of six time periods whose load margins are not satisfied with the desired load margin. Using the proposed MP-VSTS model and method, two transmission lines (line 3–5 and line 31–32) are needed to switch out from the base case, and the load margins of the whole 12 h are increased to meet the requirement.

4.2. Example 2: 662-Bus Power System

A 662-bus power system is used to verify the effectiveness of the proposed MP-VSTS method on a large-scale power system. The test system consists of 1017 transmission lines, with total loads of 25827 MW and 8364 Mvar, respectively. A total of 50 loads at buses #630–#638, #640–#645, #650–#658, #662–#668, #673–#676, #680–#683, #686–#690, #693, and #696–#700 are increased, and the rest of the loads remain unchanged. Five generators at buses #571, #572, #639, #649, and #659 are committed to supplying the increased load demands. Here, $\lambda_{th} = 3950$ MW. The load margins of the pre-switching base case of each period are shown in Figure 8.

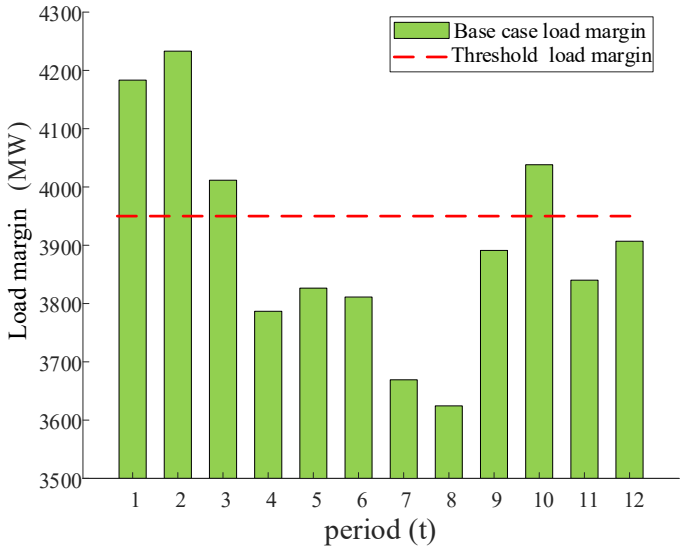

Figure 8. Load margin of pre-switching power system at each period in a 662-bus power system.

The proposed two-stage method is applied for the case at period #4. After the pre-screening stage, 56 out of 866 transmission candidates are reserved due to the positive sensitives, and the transmission candidates with the top 10 sensitivities are listed in Table 8. The iterative TS solutions of the MILP and NLP subproblems and the changes in the 0–1 integer variables are shown in Tables 9 and 10, respectively. For period #4, the switching line solutions are found after two iterations. In the first iteration of solving the MILP subproblem, six lines are selected from all the candidate lines (obtained in stage 1), and then the solutions of the MILP subproblem are sent to the NLP subproblem as the initial point. After the NLP subproblem, lines 714–727 are solved ($\overline{Z}^{1}_{714-727.4} = 0.0032$; $\Delta\overline{\lambda}^{-1}_{714-724.4} = 0.0018$). The 0–1 variable of the line 714–727 is rounded to zero according to (26) and sent to the MILP subproblem of the next iteration. During the second iteration, the

solutions of the two subproblems are converged, and line 714–727 with a load margin of 4007.65 MW is the final solution.

Table 8. Sensitivities of the top 10 lines at period #4.

Switching Lines	Sensitivity	Switching Lines	Sensitivity
697–727	6.3289	714–727	3.7150
643–698	5.1848	696–708	3.6778
687–714	4.7291	624–745	2.5994
624–625	4.3707	894–895	2.4184
641–649	3.9131	735–761	2.1806

Table 9. TS solutions of each iteration in a 662-bus power system.

k	Problem	Switching Lines
1	MILP	624–625, 643–698, 643–798, 686–708, 697–727, 714–727
	NLP	714–727
2	MILP	714–727
	NLP	714–727

Table 10. Changes in 0–1 integer variables in stage 2 in a 662-bus power system.

k	Problem	$Z_{624-625}$	$Z_{643-698}$	$Z_{643-798}$	$Z_{686-708}$	$Z_{697-727}$	$Z_{717-727}$
1	MILP	0	0	0	0	0	0
	NLP	1	1	1	1	1	0.0018
2	MILP	1	1	1	1	1	0
	NLP	1	1	1	1	1	0.0032

The load margins before and after line switching of each period are shown in Figure 9, and the status of the transmission line in each period is listed in Table 11. In this example, the load margins of periods 4–6 are increased above the desired value by switching line 714–727 out. And the load margins of periods 7–12 meet the load margin demand by switching line 624–625 out at period #7. Only two lines are needed to be switched out at periods 4 and 7 in this example.

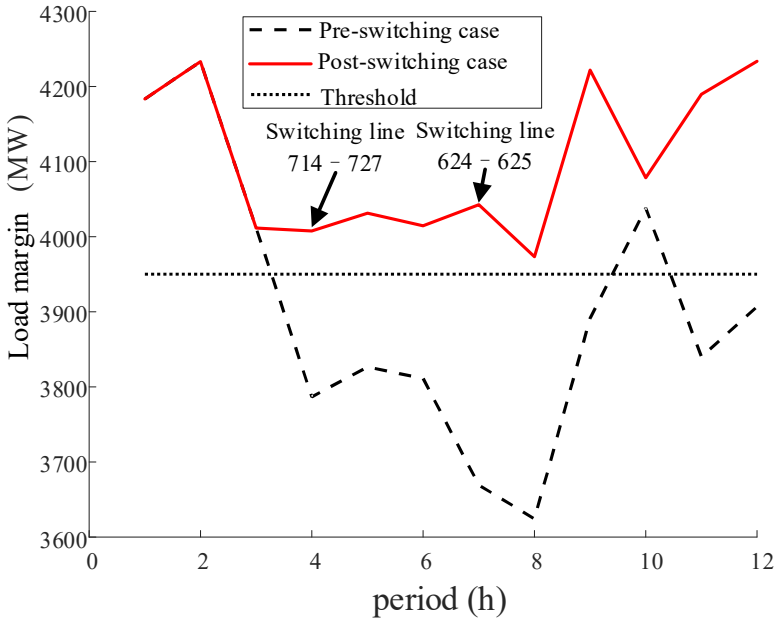

Figure 9. Load margins before and after transmission line switching for each period in a 662-bus power system.

Table 11. Transmission line switching schemes for each period of 662-bus power system.

Line	Transmission Line Status (Hour)											
	1	**2**	**3**	**4**	**5**	**6**	**7**	**8**	**9**	**10**	**11**	**12**
624–625	1	1	1	1	1	1	0	0	0	0	0	0
714–727	1	1	1	0	0	0	0	0	0	0	0	0

4.3. Comparisons with the Methods in the Literature

In this section, the proposed method is compared with the continuation power flow tool (CPFLOW) [30] and the method used in [12]. The solutions of the IEEE 118-bus system and the 662-bus power system are listed in Tables 12 and 13, respectively.

Table 12. Comparison of different methods of IEEE 118-bus system.

Period	Method	Switching Lines	λ_t^{post}/MW	Time/s
#5	Proposed method	31–32	2570.05	13.61
	Method in [12]	31–32	2570.05	121.42
	CPFLOW	31–32	2570.05	220.64
#8	Proposed method	1–2	2710.12	12.54
	Method in [12]	3–5	2624.34	78.32
	CPFLOW	1–2	2710.12	213.62

Table 13. Comparison of different methods in the 662-bus system.

Period	Method	Switching Lines	λ_t^{post}/MW	Time/s
#4	Proposed method	714–727	4007.65	30.74
	Method in [12]	714–727	4007.65	2785.64
	CPFLOW	624–625	3972.42	5573.85
#7	Proposed method	624–625	4042.48	29.89
	Method in [12]	624–625	4042.48	2548.34
	CPFLOW	624–625	4042.48	3935.03

It can be observed that (1) the proposed method can identify the same solution as that of the CPFLOW, which can be viewed as the global solution; however, the solution using the method in [12] may be different from that of the CFPLOW; (2) the total computation times of the proposed method are 13.61 s and 12.54 s, respectively, which is significantly less than that of the CPFLOW. Compared with the CPFLOW method and the method in [12], the proposed method can find effective solutions within a relatively short time, especially in large-scale power systems.

5. Conclusions

In this paper, a multi-period static voltage security and stability-constrained transmission switching problem formulation is proposed to guarantee enough voltage security and stability for each period using a rolling horizon. The proposed model considers the exact AC power flow equations and AC continual power flow equations of each time period. The distinguishing feature of the proposed MP-VSTS problem is that the requirements of both voltage security and voltage stability are considered in this paper. To solve the large-scale MINLP problem, a two-stage approach is developed, which can be decomposed into an NLP subproblem and a MILP subproblem. In addition, the TS solutions from the presented MP-VSTS method are not just the optimal solutions for a fixed time period. The effects of the TS solutions on the three future time periods are considered. The proposed model can provide a minimum number of switching actions to improve the static security and stability of power system operations. Numerical studies show the effective performance of the proposed MP-VSTS solution approach.

In this paper, the multi-period transmission switching problem is discussed. Future directions may include the co-optimization of generation redispatches, reactive power compensation, tap ratio adjustment of the transformer, and other controls. The time resolutions for the above controls may be varied and should be designed according to the characteristics of the types of controls. Hence, the topic of co-optimization of the available resources in power systems is an important future work.

Author Contributions: Conceptualization, L.W.; methodology, M.Z. and L.W.; software, J.L.; validation, M.Z.; formal analysis, K.W.; investigation, X.D.; data curation, X.D. and K.W.; writing—original draft preparation, J.L. and K.W.; writing—review and editing, M.Z. and L.W.; supervision, M.Z.; project administration, M.Z. and L.W.; funding acquisition, M.Z. and L.W. All authors have read and agreed to the published version of the manuscript.

Funding: This research was funded by the Open Fund of the National Key Laboratory of Renewable Energy Grid-integration (China Electric Power Research Institute) (No. NYB51202301633).

Institutional Review Board Statement: Not applicable.

Informed Consent Statement: Not applicable.

Data Availability Statement: The data presented in this study are only available on request from the corresponding author due to legal reasons.

Conflicts of Interest: Author Mei Zhang was employed by the company China Electric Power Research Institute. Author Jiantao Liu was employed by the company Heze Power Supply Company of State Grid, Shandong Electric Power Company. Author Xiaofan Deng was employed by the company Jiaxiang Power Supply Company of State Grid, Shandong Electric Power Company. The remaining authors declare that the research was conducted in the absence of any commercial or financial relationships that could be construed as a potential conflict of interest.

References

1. Bakhtvar, M.; Keane, A. Allocation of wind capacity subject to long term voltage stability constraints. *IEEE Trans. Power Syst.* **2016**, *31*, 2404–2414. [CrossRef]
2. Haro-Larrode, M. Variable reactance criteria to mitigate voltage deviations in power transformers in light- and over-load conditions. *Machines* **2023**, *11*, 197. [CrossRef]
3. Rolim, J.G.; Machado LJ, B. A study of the use of corrective switching in transmission systems. *IEEE Trans. Power Syst.* **1999**, *14*, 336–341. [CrossRef]
4. Hedman, K.W.; Oren, S.S.; O'Neil, R.P. A review of transmission switching and network topology optimization. In Proceedings of the IEEE/PES General Meeting, Detroit, MI, USA, 24–28 July 2011. [CrossRef]
5. Li, M.; Luh, P.B.; Michel, L.D.; Zhao, Q.; Luo, X. Corrective line switching with security constraints for the base and contingency cases. *IEEE Trans. Power Syst.* **2008**, *23*, 125–133. [CrossRef]
6. Khanabadi, M.; Ghasemi, H.; Doostizadeh, M. Optimal transmission switching considering voltage security and N-1 contingency analysis. *IEEE Trans. Power Syst.* **2013**, *28*, 542–550. [CrossRef]
7. Pineda, S.; Morales, J.M.; Porras, Á.; Domínguez, C. Tight big-Ms for Optimal Transmission Switching. *Electr. Power Syst. Res.* **2024**, *234*, 110620. [CrossRef]
8. Hedman, K.W.; O'Neill, R.P.; Fisher, E.B.; Oren, S.S. Optimal transmission switching—Sensitivity analysis and extensions. *IEEE Trans. Power Syst.* **2008**, *23*, 1469–1479. [CrossRef]
9. Hedman Kory, W.; O'Neill, R.P.; Fisher, E.B.; Oren, S.S. Optimal transmission switching with contingency analysis. *IEEE Trans. Power Syst.* **2009**, *24*, 1577–1578. [CrossRef]
10. Shao, W.; Vittal, V. Corrective switching algorithm for relieving overloads and voltage violations. *IEEE Trans. Power Syst.* **2005**, *20*, 1877–1885. [CrossRef]
11. Owusu-Mireku, R.; Chiang, H.D. A Direct method for the transient stability analysis of transmission switching events. In Proceedings of the IEEE/PES General Meeting, Portland, OR, USA, 5–10 August 2018; pp. 1–5. [CrossRef]
12. Li, C.; Chiang, H.D.; Du, Z. Online line switching method for enhancing the small-signal stability margin of power systems. *IEEE Trans. Power Syst.* **2018**, *9*, 4426–4435. [CrossRef]
13. Wang, L.; Chiang, H.D. Toward online line switching for increasing load margins to static stability limit. *IEEE Trans. Power Syst.* **2016**, *31*, 1744–1751. [CrossRef]
14. Li, B.; Zhang, X.; Zhang, Y.; Yu, Y.; Zang, Y.; Zhang, X. Optimal transmission switching based on analytical target cascading algorithm. *Front. Energy Res.* **2023**, *10*, 900462. [CrossRef]
15. Masache, P.; Carrion, D.; Cardenas, J. Optimal transmission line switching to improve the reliability of the power system considering AC power flows. *Energies* **2021**, *14*, 3281. [CrossRef]

16. Tang, S.; Li, T.; Liu, Y.; Su, Y.; Wang, Y.; Liu, F.; Gao, S. Optimal transmission switching for short-circuit current limitation based on deep reinforcement learning. *Energies* **2022**, *15*, 9200. [CrossRef]
17. Balasubramanian, P.; Sahraei-Ardakani, M.; Li, X.; Hedman, K.W. Towards smart corrective switching: Analysis and advancement of PJM switching solutions. IET Generation. *Transm. Distrib.* **2015**, *10*, 1984–1992. [CrossRef]
18. Han, J.; Papavasiliou, A. The impacts of transmission topology control on the European electricity network. *IEEE Trans. Power Syst.* **2016**, *31*, 496–507. [CrossRef]
19. Wang, L.; Chiang, H.D. Group-based line switching for enhancing contingency-constrained steady-state voltage stability. *IEEE Trans. Power Syst.* **2020**, *35*, 1489–1498. [CrossRef]
20. Wang, C.; Wang, L.; Deng, X.; Liu, J.; Guo, D. Scenario-based line switching for enhancing static voltage stability with uncertainty of renewables and loads. *Int. J. Electr. Power Energy Syst.* **2023**, *145*, 108653. [CrossRef]
21. Liu, C.; Wang, J.; Ostrowski, J. Static switching security in multi-period transmission switching. *IEEE Trans. Power Syst.* **2012**, *27*, 1850–1858. [CrossRef]
22. Fu, Y.Y.; Chiang, H.D. Toward optimal multiperiod network reconfiguration for increasing the hosting capacity of distribution networks. *IEEE Trans Power Deliv.* **2018**, *33*, 2294–2304. [CrossRef]
23. Guo, D.; Wang, L.; Jiao, T.; Wu, K.; Yang, W. Day-ahead voltage-stability-constrained network topology optimization with uncertainties. *J. Mod. Power Syst. Clean Energy* **2024**, *12*, 730–741. [CrossRef]
24. Bugaje, A.A.; Cremer, J.L.; Strbac, G. Real-time transmission switching with neural networks. *IET Gener. Transm. Distrib.* **2022**, *17*, 696–705. [CrossRef]
25. Jabarnejad, M. A genetic algorithm for AC optimal transmission switching. In GECCO'21: Proceedings of the Genetic and Evolutionary Computation Conference, Lille, France, 10–14 July 2021; pp. 973–981. [CrossRef]
26. Shi, J.; Oren, S.S. Stochastic unit commitment with topology control recourse for power systems with large-scale renewable integration. *IEEE Trans. Power Syst.* **2018**, *33*, 3315–3324. [CrossRef]
27. Flores, M.; Macedo, L.H.; Romero, R. Alternative mathematical models for the optimal transmission switching problem. *IEEE Syst. J.* **2021**, *15*, 1245–1255. [CrossRef]
28. Liu, X.; Wen, Y.; Li, Z. Multiple solutions of transmission line switching in power systems. *IEEE Trans. Power Syst.* **2018**, *33*, 1118–1120. [CrossRef]
29. University of Washington. Power Systems Test Case Archive. Available online: http://www.ee.washington.edu/research/pstca/ (accessed on 18 September 2024).
30. Chiang, H.D.; Flueck, A.J.; Shah, K.S.; Balu, N. CPFLOW: A practical tool for tracing power system steady state stationary behavior due to load and generation variations. *IEEE Trans. Power Syst.* **1995**, *10*, 623–634. [CrossRef]